CRACK BRIDGING AND TRAPPING IN BOROSILICATE MATRIX COMPOSITES WITH DISTRIBUTED METAL PARTICLES

M. Kotoul[1], I. Dlouhy[2] and T. Vyslouzil[1]
[1]Brno University of Technology, [2]Institute of Physics of Materials ASCR
[1]Dept. of Mechanics of Solids, Brno University of Technology, 616 69 Brno, Czech Republic
[2]Institute of Physics of Materials ASCR, 61662 Brno, Czech Republic
Kotoul@umt.fme.vutbr.cz

Abstract

One of the most efficient ways to improve the fracture toughness of ceramics is to reinforce them by large volume fraction of bonded metal particles (e.g., Krstic [1]; Evans and McMeeking [2]). The toughening effect of the metal particles was attributed to both crack trapping and bridging. While the bridging effect has been relatively well documented, the crack trapping effect is still somewhat inadequately understood. In contrast to crack bridging, the effectiveness of crack trapping increases with the debonding toughness of the particle/matrix interface. When the tough heterogeneities are equiaxed particles, adhesive strength becomes a very critical issue. Specifically, some optimum interface debonding is needed to remove the geometric constraint and allow the particles to deform plastically in a significant part of their volume. The aim of the contribution is to confront the measured fracture toughness values obtained on borosilicate glass matrix composites with theoretical predictions.

Introduction

The toughening of brittle solids through the inclusion of ductile phase is generally accomplished extrinsically, i.e. through the development of crack-tip shielding from crack deflection and/or crack bridging by intact ductile particles in the crack wake, e.g. [3,4]; such mechanisms invariably lead to rising R-curve behaviour (crack growth toughening) but can result in susceptibility to fatigue failure as they have a tendency to degrade under cyclic loading [3]. In the case of ceramics, glasses or intermetallics for high-temperature applications, the choice of reinforcements is limited to the refractory metals such as Mo, Nb, Cr, V and W due to their high melting temperature, although many of these refractory metal reinforcements do not exhibit significant ductility at room temperature [5]. For the effect to produce an improvement in the fracture toughness, the quality of the particle/matrix interface becomes of great importance because it strongly influences the particle deformation pattern. Specifically, some optimum interface debonding is needed to remove the geometric constraint and allow the particles to deform plastically in a significant part of their volume.

Theoretical models

When cracks encounter spherical obstacles and are trapped by them, they begin probing the strength and toughness of the interface while commencing the bowing process. Any perturbation of the crack tip away from the equator of a spherical obstacle subjects interface

to an opening mode of stress intensity. Thus any time during additional remote loading, a crack front has the option of following whatever path offers the least *local* resistance over, around, or through the obstacles. When the obstacles are cylindrical, relatively little K_I is applied to the interface if the rods are perpendicular to the crack plane, and the full level trapping-induced toughness is easily reached.

When the crack encounters an array of strongly bonded particles, the crack front will first stably penetrate between the particles, and, after the critical penetration depth is reached, overcome the trapping effect. In this process additional crack growth driving force is required due to the non-uniform distribution of the stress intensity along the verge of propagating. If the ceramics-metal bonding is strong, after the crack front overcomes the crack trapping effect, the metal particles will be left behind and bridge across the two crack flanks. Eventually with the increasing of the applied stress intensity the particles will be broken. Bower and Ortiz [6] have conducted numerical simulations of the cleavage front of crack that is trapped by tough, perfectly bonded particles. Their numerical results are closely approximated by the expression

$$\frac{G_{IC}^{trap}}{G_{IC}} = \left(\frac{K_{IC}^{trap}}{K_{IC}}\right)^2 = 1 - 2\left(\frac{3f}{4\pi}\right)^{1/3} + \left[2.1 + 4.8\left(\frac{3f}{4\pi}\right)^{1/3}\right]^2 2\left(\frac{3f}{4\pi}\right)^{1/3}, \text{ for } 0 < f < 0.18, \quad (1)$$

where G_{IC}^{trap} is the maximum remote energy release rate required to bypass a single row of particles, G_{IC} stands for the matrix toughness and f for the volume fraction of particles. After the crack front overcomes the crack trapping effect, the particles will be left behind and bridge the crack. Bower and Ortiz [7] suggest that for bridging particles to form, the particles toughness, G_{IC}^{part}, should exceed $G_{IC}^{part}/G_{IC} \geq [2.1+4.8(3f/4\pi)^{1/3}]^2$. If this is not the case, the crack cut through the particles and the maximum possible toughness of the composite is

$$\frac{G_{IC}^{eff}}{G_{IC}} = 1 + 2\left(\frac{3f}{4\pi}\right)^{1/3}\left(\frac{G_{IC}^{part}}{G_{IC}} - 1\right). \quad (2)$$

If the particle toughness is comparable to that of the matrix, very little improvement in toughness is observed. Xu *et al*. [8] have shown that if the particles debond from the matrix the crack front bypasses a row of particle more easily leaving debonded particles in its wake. They have also shown that interfacial debonding considerably reduces the effectiveness of crack trapping and the improvement in toughness is then well approximated by

$$\frac{G_{IC}^{trap}}{G_{IC}} = 1 + 4.23\left(\frac{3f\sqrt{\pi}}{4}\right)^{1/3}\left(\frac{G_d}{G_{IC}} - 0.15\right), \quad (3)$$

where G_d is the interface debonding toughness. Note that the prediction according to Eq. (3) holds if $G_{IC}^{part} > 4G_d$, $0.2 \leq G_d/G_{IC} \leq 1$ and $0 \leq f \leq 0.19$. The crack front repeatedly overcomes the crack trapping effect, leaving debonded particles in its wake. Several hundreds rows of bridging particles may form in this way. A three dimensional analysis of this process would be prohibitively expensive, thus a simple two dimensional model is usually accepted to estimate the influence of bridging particles. Provided that the bridging zone is much longer

than the spacing between particles, it can be idealised as a distribution of pressure $\sigma_0(\Delta)$ acting on the crack faces and thus reducing the energy release rate uniformly over the propagating crack front. Δ denotes the crack opening displacement. One may calculate this reduction using the *J* integral as

$$\Delta G_{IC}^{bridg} = \int_0^{\Delta_c} \sigma_0(\Delta) d\Delta, \quad \text{with } \Delta_c \text{ standing for critical value.}$$

(4)

The effective toughness of composite follows then as $G_{IC}^{eff} = G_{IC}^{trap} + \Delta G_{IC}^{bridg}$. To evaluate ΔG_{IC}^{bridg}, one must find the cohesive law $\sigma_0(\Delta)$. A number of attempts have been made to analyse the plastic stretching of a plastically deformable particle within elastic medium, using slip line fields [2], finite elements [9] and analytical approximations [10]-[12], all with the objective of relating the stress/crack opening relation $\sigma_0(\Delta)$ to the uniaxial plastic flow properties of the ductile material. The fact that partial debonding can increase the total plastic work dissipated in particles was found in model experiments by Ashby *et al*. [13]. A simple approximate analysis for the effect of partial debonding on the work of separation was proposed by Bao and Hui [10] based on assuming circular neck shapes and using Bridgman approximation for the stress in the neck. Tvergaard [9] performed a detailed finite element analysis of ductile particle debonding during crack bridging in ceramics. He employed plastic strain controlled model of debonding. His numerical results have shown that the average tensile stress obtained by Bridgman approximation in [10] is underestimated and thus the numerical estimate of the dissipated plastic work in ductile particle is higher than that obtained by rigid-plastic model [10]. The rigid-plastic model can be improved using suggestions made by Rubinstein [11]. Specifically, the particle is assumed to develop a neck of parabolic profile which is a simplified version of that obtained be Tvergaard using finite element computations, see Fig. 1.

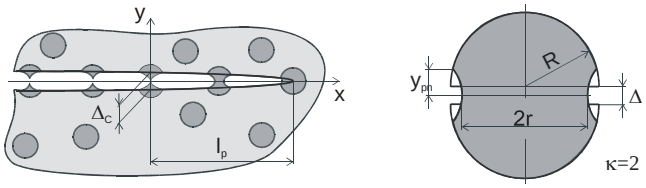

FIGURE1: Scheme of bridged crack and particle deformation shape.

The current radius of the bridging cross section of a particle *r*, the vertical coordinate of the intersection of the parabolic neck with the undisturbed spherical portion of a particle y_{pn} and the half of the crack opening displacement at the particle site $\Delta/2$ within the bridging zone are then related by

$$\frac{r}{R} = \sqrt{1 - \left(\frac{y_{pn}}{R} - \frac{\Delta}{2R}\right)^2} - \frac{\kappa}{2}\left(\frac{y_{pn}}{R}\right)^2,$$

(5)

where parameter κ specifies the curvature of the chosen parabolic profile in the coordinate system *x'*,*y* with its origin in the particle centre $x'/R = \kappa/2(y/R)^2 + r/R$. κ is associated with

the strength of the particle/matrix interface. The requirement of incompressibility of the particle provides then the additional condition for determination of r, y_{pn} and Δ

$$\left(1-\frac{y_{pn}}{R}+\frac{\Delta}{R}\right)^2\left(1+\frac{y_{pn}}{R}-\frac{\Delta}{R}\right)+3\left[\frac{\kappa^2}{20}\left(\frac{y_{pn}}{R}\right)^2+\frac{\kappa}{3}\frac{r}{R}\left(\frac{y_{pn}}{R}\right)^3+\frac{y_{pn}}{R}\left(\frac{r}{R}\right)^2\right]=2. \tag{6}$$

The vertical coordinate of the intersection of the parabolic neck with the undisturbed spherical portion of a particle y_{pn} can be eliminated between Eqs. (5) and (6). The resulting equation can be solved numerically to obtain the normalised bridging cross section r/R as a function of the normalised crack opening displacement Δ/R. If a power law hardening material is assumed, then the flow stress σ_f is related to the tensile strain e by $\sigma_f/\sigma_y = (e/e_y)^n$ and σ_y and e_y are the initial yielding stress and strain respectively and n is the hardening coefficient. The tensile strain e relates to the initial particle radius and to the current radius of bridging cross section by $e = 2\ln(R/r)$. Kotoul and Vrbka [12] estimated the restraining stress σ_0 using the Bridgman approximation as

$$\sigma_0 = 2^n\sigma_y e_y^{-n}\left(\frac{3f\sqrt{\pi}}{4}\right)^{2/3}\left[\ln\left(\frac{R}{r}\right)\right]^n\left(\frac{r}{R}\right)^2\left(1+\frac{2R}{\kappa r}\right)\ln\left(1+\frac{\kappa r}{2R}\right). \tag{7}$$

If the numerical relation r/R-Δ/R calculated from Eqs. (5) and (6) is substituted into Eq. (7) a desired relation of the restraining stress σ_0 associated with crack opening displacement Δ/R is obtained, see Fig. 2.

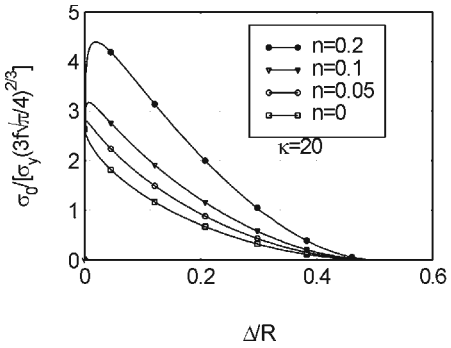

FIGURE 2.Normalised restraining stress vs normalised crack opening displacement for several values of the hardening coefficient n and the neck curvature $\kappa = 20$.

Eventually, substituting (7) into Eq. (4) one can calculate the reduction in the energy release rate. Numerical results are presented in Fig. 3 together with values obtained by Tvergaard using FEM for $e_y = 0.005$.

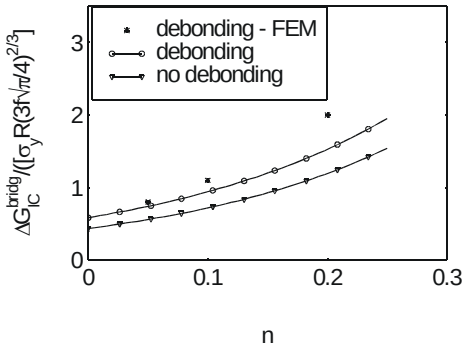

FIGURE 3: The reduction in the energy release rate vs strain hardening. Curves correspond to rigid-plastic models. The curve for no debonding is based on [].

Apparently, a significantly higher increase of the fracture toughness is predicted by the more accurate numerical computations than by the rigid-plastic models. It is important to note that the additional fracture toughness due to ductile particle bridging increases with the particle size R as well as the yield stress σ_y and the volume fraction f of the ductile particles. When ductile rupture involves hole nucleation and growth, the form of the stress/displacement law is basically unchanged, but R then becomes the half-spacing between voids. The void spacing is thus the scale parameter that dictates the toughening.

The interfacial failure may occur either by cracking in the brittle matrix near the interface or by separation of the ductile particle from the hard ceramic matrix. The latter mechanism can be controlled by plastic strain which is represented approximately by gradually reducing the maximum interface stress σ_{max} when the effective plastic strain at the interface exceeds a critical value. Actually, Tvergaard [9] used such a model. He found that for constant interface strength no partial debonding is predicted. More specifically, for $\sigma_{max} = 5\sigma_y$ a very small debonding was observed starting from the intersection with the brittle matrix crack. On the other side, for $\sigma_{max} = 3\sigma_y$ debonding starts at the pole of the spherical particle, leading to complete interfacial separation of the particle. However, when the plastic strain controls a failure mechanism, partial debonding is predicted and the found debonding lengths fall within the range of values observed experimentally.

Kotoul and Vrbka [12] used an approach based on the energy considerations to estimate the length h of debonded interface of a particle in the vicinity of crack tip under assumption that $h << R$ i. e. for a relatively strong interface. Due to mechanical constraint a nonzero axial plastic strain increment is then observed only in a thin layer of thickness $\approx 2h$ as it can also be documented by FEM simulation of the deformation of the particle constrained by elastic matrix. The aim is to calculate the potential energy loss $-\delta\Pi$ associated with the growth of thickness of the debonded layer δh. The energy supply is partly dissipated by plastic work in the debonded layer δW_p and partly is absorbed in the mechanism of particle/matrix interface debonding. The energy release rate relation

$$2\pi R G_d + \frac{\delta W_p}{\delta h} = -\frac{\delta \Pi}{\delta h} \tag{8}$$

provides the condition governing the debonding length h. To display results obtained from Eq. (8) in a dimensionless form it is expedient to introduce a dimensionless composite parameter $k = K_{IC}/(2\sigma_y\sqrt{(2R)})$ which combines the fracture toughness of the matrix K_{IC} with the yield strength σ_y and the radius R of particles. Refer to Fig. 4, which displays a relation

between the ratio h/R versus the ratio of debonding to fracture matrix toughness G_d/G_{IC}. Note that h/R is not a single-valued function of G_d/G_{IC}. The upper part of each curve represents stable debonded lengths, but for debonding to occur at all an energy barrier associated with the region between the horizontal axis and each lower branch must be overcome. The results in Fig. 4 indicate that there exist threshold values $(G_d/G_{IC})^*$ such that for $G_d/G_{IC} > (G_d/G_{IC})^*$ debonding can not occur. The threshold value $(G_d/G_{IC})^*$ depends on the composite parameter k and on the particle volume fraction f. Fig. 5 summarizes threshold values $(G_d/G_{IC})^*$ as a function of the composite parameter k for several values of f that would prevent debonding. Note that for a constant value of the matrix fracture toughness the composite parameter k increases with decreasing particle yield stress and/or particle size. As a consequence, threshold $(G_d/G_{IC})^*$ increases with a decrease of the particle yield stress and/or particle size.

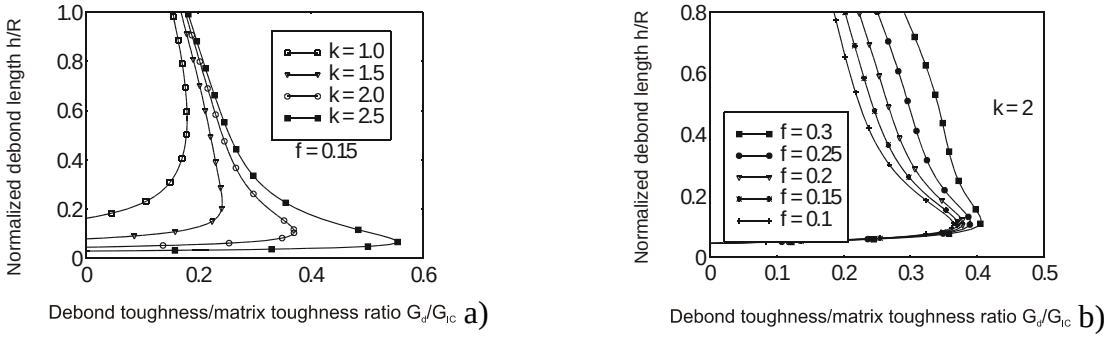

FIGURE 4: a) Debond length vs debonding-toughness/matrix-toughness ratio for several values of the composite parameter k and the particle volume fraction f=0.15. b) Debond length vs debonding-toughness/matrix-toughness for several values of the particle volume fraction f and the composite parameter k=2.

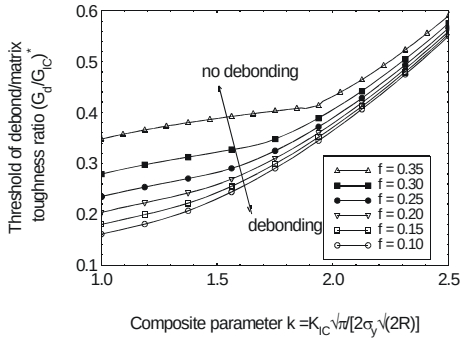

FIGURE 5. Threshold value $(G_d/G_{IC})^*$ as function of k for several values of f.

Comparison between theory and experiment

Dlouhy et al. [14] observed that experimental values of the fracture toughness of borosilicate glass reinforced by vanadium or molybdenum particles, their shape can roughly be treated as spherical one, have fallen far behind to the theoretical expectations of the enhancement of fracture toughness according to the crack bridging view. The physical properties and further relevant information on the borosilicate glass/vanadium particle composite are given in Table 1. Specifically, the experimentally found toughening ratio K_{IC}^{eff}/K_{IC} (composite toughness/matrix toughness) was 1.4 for the volume fraction f=0.1 of vanadium particles while the theoretical prediction based on the crack bridging model according to Eq. (4) is

more than one order higher. When the observed particle cleavage in about 85 vol % of the metal inclusions was taken into account, the theoretical prediction of the toughening ratio somewhat decreases but still amounts about 5 times higher value. This estimate is further reduced to the value about of 2 if the existence of impurities in the particles with 2R > 10 μm is taken into account. It was found that the mean half-spacing between these impurities is about of 2.2 μm. The impurities can act as void nucleating features and, as it was already pointed out, void spacing becomes the scale parameter that dictates the toughening. This is in agreement with finding that extensive stretching was not detected and the large scale bridging was observed to occur only to a small extent. It is then, however, rather dubious to idealise bridging particles as a distribution of pressure $\sigma_0(\Delta)$ acting on the crack faces. It should be noted that the observed particle cleavage, see Fig. 6, indicates a decrease in particle plasticity induced due to two causes: (i) constraints imposed by the rigid matrix and (ii) embrittlement due to the high-temperature fabrication process. Observe in Fig. 2 that the peak stress in particles can reach a value about of 4 times higher then the yield stress. Apparently, as the yield stress increases the peak average stress can attain a critical value for the onset of cleavage.

TABLE 1. Selected material properties of constituents

	Borosilicate glass DURAN	Mo- particles	Borosilicate glassVG98	V - particles
Average particle size [μm]	8	< 3	5.5	12
Thermal expansion coeff. α [K^{-1}]	3.3	5.1	10.6	9.7
Young's modulus *E* [GPa]	63	336	74.8	124
Poisson ratio ν	0.22	0.31	0.23	0.36
Fracture strength [MPa]	56	466	48	540
Yield strength [MPa]		437		
K_{IC} [MPa√m]	0.6	31	0.7	

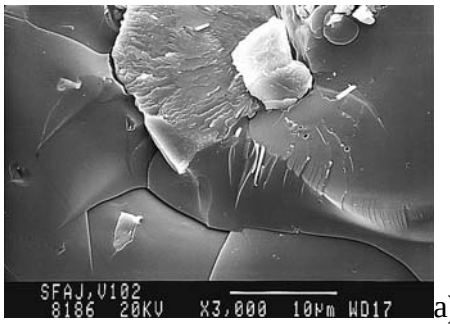

a)

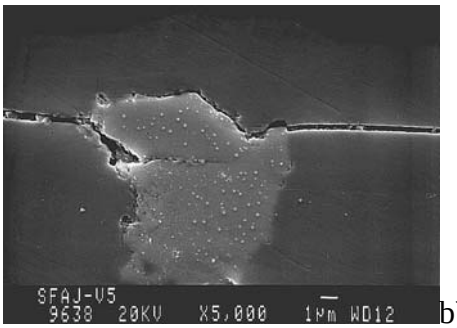

b)

FIGURE 6: a) Details of V-particle as observed on fracture surface. b) Cross section of crack in V-particle and partial debonding. Crack propagates from left to the right.

So far no contribution from crack trapping was included. Let us first discuss the model of crack that is trapped by tough, perfectly bonded particles described in Eq. (1). This model predicts the toughening ratio $K_{IC}^{trap}/K_{IC} = 2.7$ for $f = 0.1$. It is seen that this value is far above the experimental value. Apparently, the model has to be rejected. Consider now the crack trapping model for the case when particles debond from the matrix. The improvement in

toughness is then approximated by Eq. (3). The critical issue in Eq. (3) is the estimate of the ratio G_d/G_{IC}. The relation (3) requires that for the experimental value of toughening $K_{IC}^{eff}/K_{IC}=1.4$ and the volume fraction f = 0.1 the ratio G_d/G_{IC} should be less then 0.6. This value is in accordance with the threshold values $(G_d/G_{IC})^*$ predicted in [12], see Fig. 4. Note that the work of separation per unit interface area according to the debonding model used by Tvergaard [9] is $9\sigma_{max}\delta_n/16$, where δ_n stands for final separation. The effect of plastic strain controlled failure of the interface is represented by gradually reducing interface stress σ_{max}. If the average value of σ_{max} is estimated as $2.5\sigma_y$, $G_{IC} \approx 2\gamma_m$, where γ_m =3.1 J/m^2 is the surface energy of the borosilicate glass VG98, the final separation should comply with the inequality $\delta_n \le 2.65/\sigma_y$. For σ_y = 450 MPa very small values result, i.e. $\delta_n \le 5.9$ nm. Let us now substitute the threshold values $(G_d/G_{IC})^*$ into Eq. (3). Because $(G_d/G_{IC})^*$ depends on f, the improvement in toughness K_{IC}^{trap}/K_{IC} can be plotted against f for various values of the composite parameter k, see Fig. 7. Apparently, this trapping model provides best agreement with experimental data. Note that Xu *et al*. [8] stated that the model is likely to underestimate the true effective toughness by about 10%. Also note that bridging particles remaining in the wake are likely in the regime of "unstable bridging", i.e. they fracture before the crack front reaches the second row of obstacles.

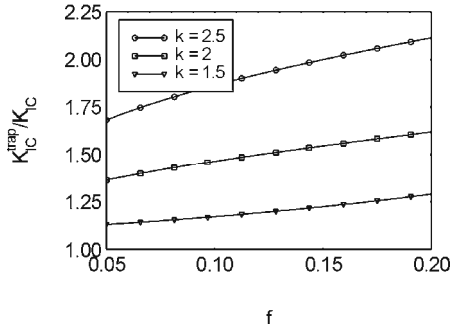

FIGURE 7: The improvement in toughness K_{IC}^{trap}/K_{IC} vs f for various values k.

References

1. Krstic, V.D., *Phil. Mag*., vol **A98**, 695-708, 1983.
2. Evans, A.G. and McMeeking, R.M., *Acta Metall*., vol **34**, 2435-2446, 1986.
3. Ritchie, R.O., *Int. J. Fracture*, vol **100**, 55-83, 1999.
4. Chan, K.S., *Metall. Trans. A*, vol **23A**, 183-199, 1992.
5. Davidson, D.L., Chan, K.S. and Anton, D.L., *Metall. Mater. Trans. A*, vol **27A**, 3007-3018, 1996.
6. Bower, A. F. and Ortiz, M., *J. Mech. Phys. Solids*, vol **39**, 815-858, 1991.
7. Bower, A. F. and Ortiz, M., *J. Eng. Mat. Technology*, vol **115**, 228-236, 1993.
8. Xu, G., Bower, A. F. and Ortiz, M., *J. Mech. Phys. Solids*, vol **46**, 1815-1833, 1998.
9. Tvergaard, V., *Int. J. Mech. Sci*., vol **34**, 635-649, 1992.
10. Bao, G. and Hui, C.-Y., *Int. J. Solids Struct*., vol **26**, 631-642, 1990.
11. Rubinstein, A.A. and Wang, P., *J. Mech. Phys. Solids* vol **46**, 1139-1154, 1998.
12. Kotoul, M. and Vrbka, J., *J. Theoret. Appl. Fract. Mech*.,vol **40**, 23-44, 2003.
13. Ashby, M.F., Blunt, F.J. and Bannister, M., *Acta Metall*., vol **37**, 1847-1857, 1989.

14. Dlouhy, I., Reinisch, M., Boccaccini, A.R. and Knott, J.F., *Fatigue Fract. Engng. Struct*., vol 20, 1235-1253,(1997).

The support trough the grant GACR 101/02/0683 and the project No. MSM 262100001 is acknowledged.